optics] Metrology of the 1 Jubble Space Telescope Simulator
by means of 1 Iartmann Tests

Arthur 11, Vaughan and Robert P. Korechoff

Jet 1 'ropul sion I aboratory
California 1 nstitute of Technology
Pasadena, California 91109

ABSTRACT

This paper describes the use of a Hartmann-ty pe pupil mask and CCD camera to perform wavefront and focus validation of the Hubble Space Telescope simulator before and during environmental testing of the second-generation Wide]{'icddmd Planetary Camera. The method yields a focus accuracy at F/24 of about ±100 m icrometers even in the presence of 3.5 waves of spherical aberration. The method avoids the introduction of potentially imperfect auxiliary optical tooling (e.g., null correctors).

1. OVERVIEW

A reliable way to characterize the wavefront produced by an optical system is through the use of the classical Hartmann test[1], in which the paths of light "rays" defined by holes in a mask are deduced from measurements of their intercepts with planes at known positions near a focus. Although originally devised for testing nearly aberration-free telescope objectives, the Hartmann test readily lends itself to testing of highly aberrated systems whose evaluation by means of interferometry would require a null corrector. This is exactly the situation that arises in the "Stimulus" used in testing the second-generation Wide Field and Planetary camera (WFPC-2) for the] Jubble Space Telescope (J Is'J'). The Stimulus was built to simulate the optical syst em of the 1 IST including about 3.5 waves rms of spherical aberration. It serves as the primary gage of the optical quality of the W FPC-2 instrument prior to launching of the instrument and installation into HST[2].

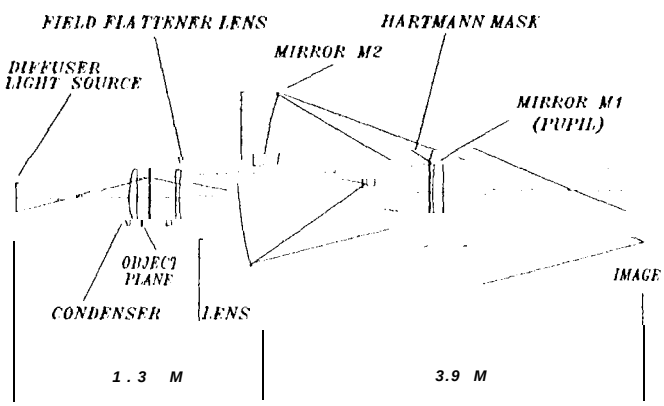

SCHEMATIC OPTICAL LAYOUT

Fig. 1. Hubble Space Telescope simulator ("Stimulus") for the second-generation Wide Field/Planetary Camera.

The Hartmann test is one of several methods for deducing the optical prescription of a system by analysis of imperfectly focused images. Another approach to "prescription retrieval" is to vary the parameters of an assumed complex pupil function so as to m ini - mize the difference between the computed diffraction point Spread function and the observed one! [3,4]. A technique closely related to the] Hartmann test reconstructs the curvature O f a wavefront by solving a differential equation for the brightness distribution in out-of-focus images[5]. The latter method works well only when diffraction effects do not cont ribute signifi - cantly to the out-of-focus im age struct ure. The classical Hartmann test introduces a very sin]- ple, accurately known real pupil function with symmetrical features (the mask with holes). Diffraction mfry or refry not contribute si~nificantly to the out-of-focus image structure in a Hartmann test (depending upon wavelength). Because the diffraction by circular bolos is symm etrical, t he centroids of light bundles passing through them can usually be assumed to define ray paths t hat can be accurately described in terms of geometrical optics. J Diffraction simulation shows that to wel I within t he accuracy of our measurements this assumption remains valid in the presence of the spherical aberration exhibited by t he HST and simulated by the Stimulus.

2. BASIC Al'l'l{OAC] 1

The optical layout of the WFPC-2 Stimulus is shown schematically in Fig. 1. The optical system produces a virtual image of M_1 at a distance of 700 cm from the image plane, thus coinciding with the virtual image of the primary mirror (i. e., the entrance pupil) of the 11,S'1'. The pupil de-magnification at M, (pupil image size at M,-: primary mirror size) is m = 0,0203. The 11 artmann mask is located about 0.1 mm ahead of the vertex of M_1. The masks were fabricated by precision chemical etching of 0.0) 0 inch thick (0,254 mm) beryllium copper flat sheet stock. The patterns used are shown in Fig. 2. *Two* patterns were employed. The first. is a rectangular pattern of 36 holes. The second is a pattern of 8 opaque disks (equal in size to the holes of the first pattern) supported by 4 thin radial spokes. The first pattern is a standard 1 lartmann screen in which the evenly spaced bolos represent essentially equal fractions of the pupil area, The second pattern makes use of the fact that diffraction by a circular obstacle gives rise to a bright spot (as first demonst rated in the 19th century by Arago[6]) at the center of its dark shadow. The utility of the second pattern is that it interferes negligibly with the optical perform ance of the Stimulus; it can thus be left in place to enable Stimulus focus verification during tests of WI'']'C-2.

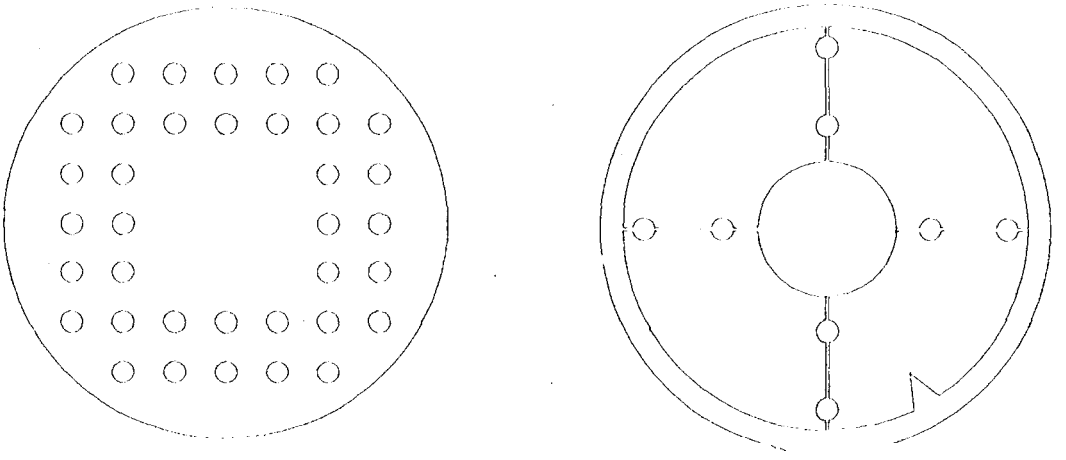

Fig. 2. Hartmann mask at left contains 36 holes. "Arago" mask at right provides a central obscuration and 8 accurately circular opaque disks supported by 0.254. mm-wide spokes. Bright spots at the centers oft he shadows of the disks are used to monitor focus. Masks are shown approximately actual size.

To allow the out-of-focus images to fill a convenient format on our detector (a I oral 800 x 800" CCI) wit h 15 micron pixels), the det ector is located at an accurately known position about A = 20 cm beyond the pa raxial focus of the Stimulus. In the case of the 11 artmann mask, the hole size d was chosen to minimize the size of the blur circle caused by the combination of defocus and diffraction. This occurs when t he two contributions are made approx i mat ely equal, so that

$$d = mf\sqrt{(2.4\lambda/\Delta)} = 3.2 \text{ mm},$$

where f = 57600 is the effective focal length of the I 1S1' F/24 Ritchey-Chretien focus and λ = 632 nm. The blur circle size al the detector is then approximately

$$2.4(\sqrt{2})\lambda fm/d = 0.78 \text{ mm (52 pixels)}.$$

The spacing between holes (and hence the number of holes) in the Hartmann mask was chosen to avoid overlapping of the blur circles from adjacent features.

In the case of a circular obstacle, the bright spot of Arago can be considered to arise from a line source at the obstacle's perimeter (in accordance with Huygens' principle), or equivalently from the Fresnel zone lying just outside the perimeter. The resulting bright spot is smaller than the Airy disk produced by a circular hole of the same size, and is given approximately (for d = 3.2 mm) by

$$\lambda fm/d = 0.27\ mm\ (18\ pixels).$$

The size of the dark shadow of the obstacle can be expected to be approximately that of its geometrical shadow corresponding to the out-of-focus distance A, or slightly larger if the effect of Fresnel diffraction is taken into account. These estimates are in good accord with our experimental results as may be seen from examination of Fig. 3. Simulated patterns in excellent agreement with the observed ones have been computed with a FFT algorithm developed by C. Burrows[7].

3. INTERPRETATION OF CENTROID DATA

The Hartmann test measures slope errors. We derive slope errors from the difference between the observed detector coordinates (ξ_{obs}, η_{obs}) of the centroid of a blur circle and the position $(\xi_{calc}, \eta_{calc})$ predicted by ray tracing using the nominal optical prescription of the system including the appropriate value of Δ. The wavefront vector slope error Ψ_i corresponding to the location of the *i*th hole has the components

$$\Psi_{i,x} = (\xi_{i,obs} - \xi_{i,calc})/(f+\Delta),\quad \Psi_{i,y} = (\eta_{i,obs} - \eta_{i,calc})/(f+\Delta).$$

The analysis of vector slope error data might be done in many ways, The method we used is presented as one possible approach, 1 t is convenient to represent the wavefront by a Zernike polynomial in a circle of unit radius in rectangular coordinates (*x*, y), although the Zernike polynomials are no longer an orthonormal set when merely summed over the finite number of points defined by a Hartmann mask. The *x* and y components of slope errors corresponding to tilt, focus, and third order spherical aberration are given by first derivatives of the Zernike terms, thus:

$J_1 = 2$	*x-tilt*
$J_2 = 4x\sqrt{3}$	*x-focus*
$J_3 = (24x^3 + ,24x? - 12x)\sqrt{5}$	*x-spherica*
$J_4 = 2$	*y-tilt*
$J_5 = 4y\sqrt{3}$	*y-focus*
$J_6 = (24y^3 + 2413C>P - 12y)\sqrt{5}$	*y-spherica*

The inclusion of higher order terms would not be justified with a mask containing only 36 holes. The total tilt error at the *i*th position is represented by

We aim to select the coefficients o_j so as to minimize

$$\chi^2 = \sum (J_i - Q_i)^2.$$

The standard least squares solution is then given by the vector $[a_k]$,

$$[a_k] = [M_{kj^{-1}}][b_j],$$

where the measurement vector has the components

$$b_j = \sum \psi_i J_j(x_i, y_i),$$

and the matrix to be inverted is

$$M_{kj} = \sum J_k(x_i, y_i) J_j(x_i, y_i).$$

Note that for a symmetrical aberration (e.g. focus, spherical), the x and y components of the slope vector are linearly dependent. Consequently, inversion of the full 6 by 6 matrix M will not be possible (except when the symmetry is removed by measuring errors). The difficulty is avoided by solving for the x and y components separately using 3 by 3 matrices, in the case of symmetrical aberrations, the difference between the x and y solutions (which should in principle be identical) gives an estimate of the accuracy of the solution.

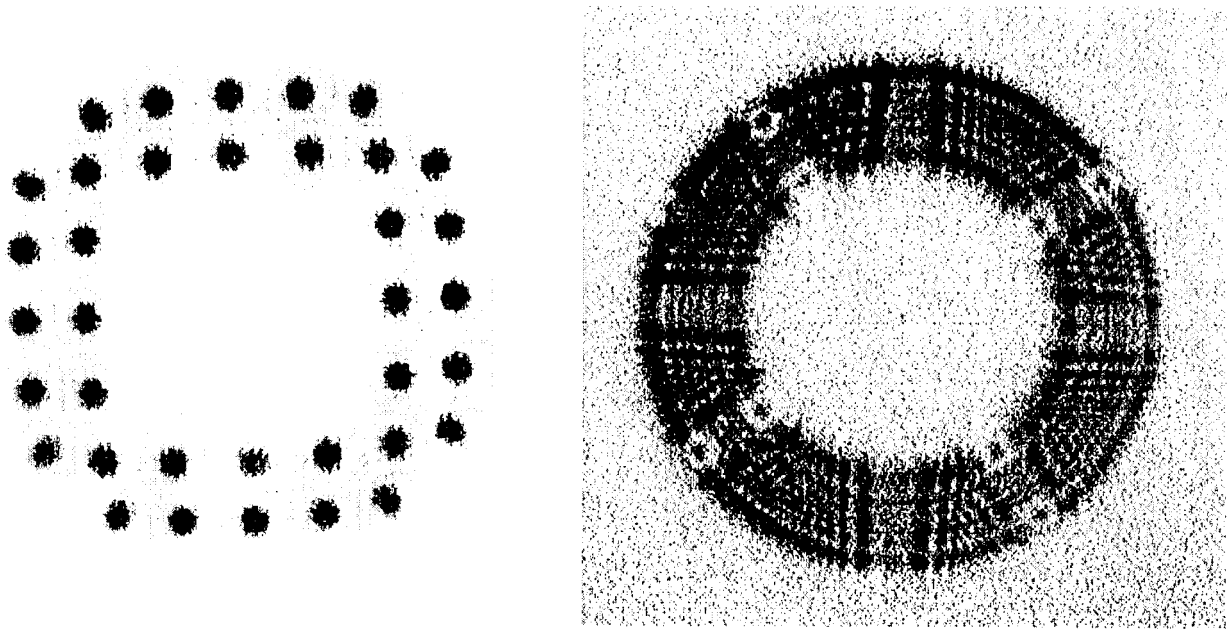

Fig. 3. Negative prints of out-of-focus diffraction patterns created by the Stimulus with the classical 1 lartmann mask (left), and "Arago" mask (right), whose forms are shown in Fig. 2. The illuminant has 5 nm bandwidth at 633 nm. The detector is a] oral 800x800 CCD with 15 micron pixels. The nearly vertical and horizontal diffraction features in the Arago pattern are caused by the secondary support vanes of the Stimulus cassegrain relay; the features oriented at about 50 degrees clockwise are produced by the mask. Note relative sizes of the Airy and Arago patterns as discussed in text.

Finally, the coefficients a_j must, in this application, be interpreted not in the usual terms of rms wavefront error, but in terms of P-V errors according to the definit ions of the polynomial used. 1 n the case of focus error, the linear shift is given by

$$\delta\Delta = 16\sqrt{3}\,F^2 a_2 \quad \text{or} \quad 16\sqrt{3}\,F^2 a_5 \quad \text{or} \quad 8\sqrt{3}\,F^2 (a_2 + a_5).$$

Solution of the equations described was performed in near-real t ime during environmental t est ing using a computer spreadsheet (1 otus 1 -2-3) which supports matrix operat ions.

4. GEOMETRICAL OPTICS MODEL

The optical prescription of the Stimulus[2] was ray traced to predict the intercepts ξ_{calc}, η_{calc} at the detector. For an axially symmetric system, only a radial fan of rays need be traced, from which the ratio of ray height at the detector to ray height, at the Hartmann mask can be computed as a function of ray height at the mask, In the Stimulus this function can be approximate by a 6th-order even-powered polynomial, which is then used to calculate intercepts for the array of rays corresponding to the Hartmann mask,

in the present application the Hartmann screen is located mar the vertex of the mirror element M_1, which forms the entrance pupil. Since this mirror is convex, a bundle of rays passing through a hole in the screen and reflecting from Ml will, in general, suffer some vignetting in passing a second time through the same hole. The situation is sketched in Fig. 4.

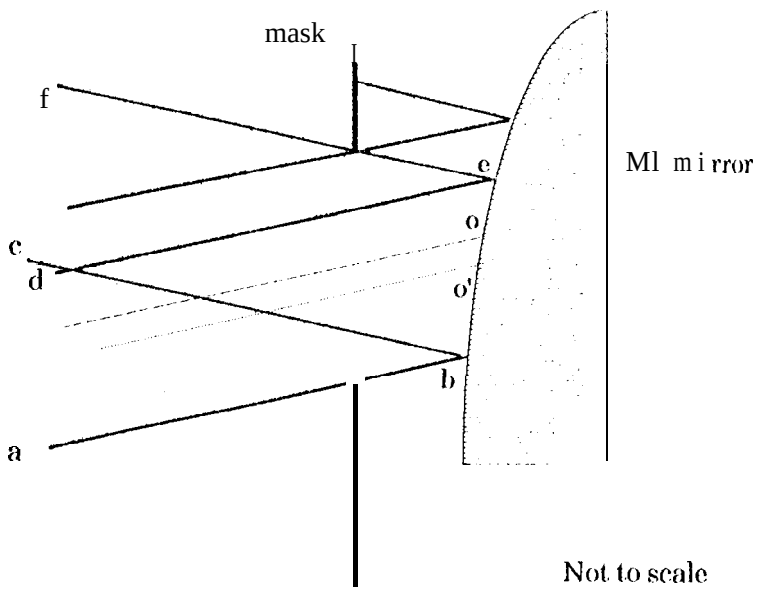

Fig. 4. Geometrical correction for vignetting by plano Stimulus Hartmann mask in front of convex mirror M1.

The ray **abc** represents the lower edge of a bundle passing the Hartmann mask from left to right. The ray **def** represents the extreme ray that just makes it back out through the same hole. The center of the original beam interects M_1 at **o**; the center of the vignetted beam intercepts M_1 at **o'**, slightly below **o**.

By raytracing a fan of rays to determine their intercepts at the mask before and after reflection by M 1, we determined the displacement, Ay, between the before and after intercepts as a function of **y**. By a method of successive approximation, we then calculate the ray **def**. For the Stimulus the resulting shift of the centroid as a function of ray height can be approximated by a power law,

$$\Delta y \approx -0.00033\ (yd/do)c'6\ cm.$$

The correction is evidently at most about 3.3 microns at the outer extreme of the pupil, This is essentially negligible, but is taken into account to eliminate any possible bias in focus or spherical aberration derived from Hartmann tests of the Stimulus.

5. RESULTS

The analysis of a typical single exposure using the Hartmann test on the WFPC-2 Stimulus is shown in Fig. 5. Plotted are the radial components of the slope errors calculated directly from measured centroids of the 36 individual spots (square symbols). A straight, line indicates the radial derivative of the Zernike focus term fitted by least squares, for a defocus of 5.79 mm relative to the nominal focus. Diamond symbols indicate the radial derivative of the Zernike spherical aberration term fitted by least squares, relative to the nominal (non-zero) spherical aberration of the Stimulus.

From analysis of repeated exposures using the 11 artmann mask, we find that the focus offset derived by the methods outlined in this paper are repeatable to within a standard deviation of about ± 0.005 inch (0. 127 mm). This is adequate to meet our conservative focus tolerance of ± 0.25 mm, To avoid systematic effects caused by pixelization, we typically move the pattern by a arbitrary dist ance on the detector between successive exposures. Almost the same results are obtained whether the spot centroids are estimated by eye (using a cursor in a video display of images), or computed by a centroiding algorithm. In either case, the 1 lartmann spot centroids are uncertain to within at least 1 or 2 pixels., primarily because of the structure introduced by interference between the multiplicity of holes in the mask when nearly coherent illumination is used. This structure disappears with white light illumination, and the measuring uncertainty is correspondingly reduced. Comparison between results obtained with white light and coherent light indicates that the observed interference structure does not introduce systematic error at a significant level.

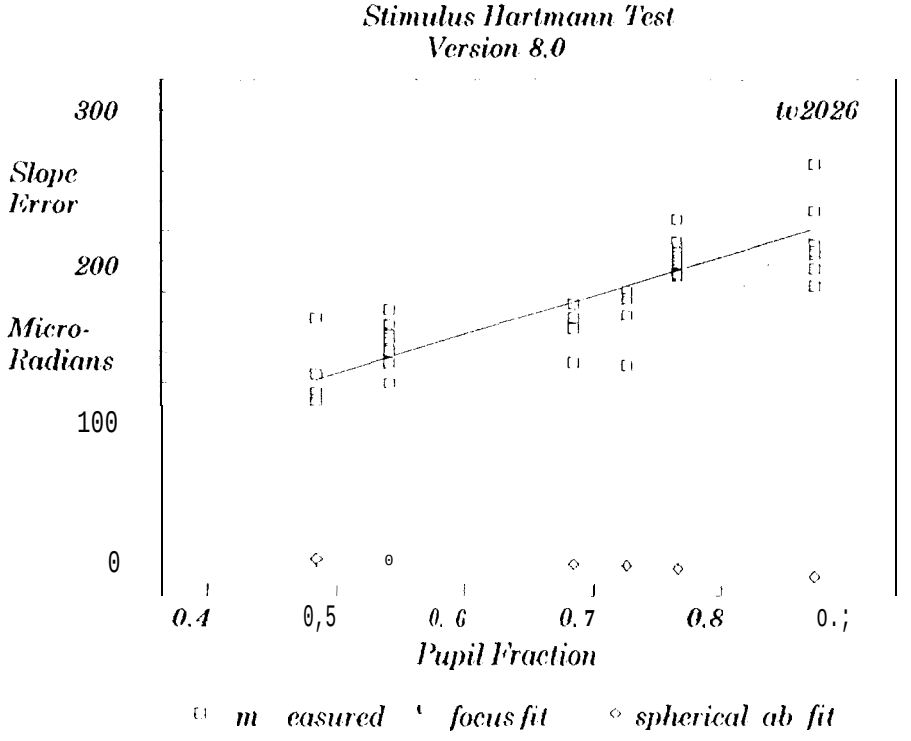

Fig. 5. Sample test result for WFPC-2 Stimulus.

The fringe structure is absent from {he! Arago spots produced by circular obstacles, perhaps in part because the obstacles are few and widely spaced. Moreover, since the Arago spots less than half as large as the Airy disks produced by circular holes of the same size, t heir centroids can be est imated with correspondingly greater precision. our analysis indicates that the focus offsets derived from the Arago mask from repeated exposures have a standard deviation essentially equal to that given by the 1 lartmann mask, although the latter

has 4.5 times as many holes. For this reason particularly, a mask consisting of an array of accurately circular obstacles could be preferable to a classical Hartmann screen in some applications.

In the application under discussion, the WFPC-2 Stimulus was initially focused visually with laser illumination using a null lens and a microscope to set the axial distance between the corrected image and a reference reticule in the WFPC-2 Radial Instrument Alignment Fixture, to within an estimated uncertainty of about 30,005 inch. The Hartmann test (in which the Stimulus is modeled both with and without the null ions) showed that the null lens actually introduces a focus shift of about 0.025 inch. A final focus correction was then made to correct for this shift, thus bringing the Stimulus to the desired focal offset relative to the reference reticule. Thus the Hartmann test (without null lens) provided the principal gage of the Stimulus focus. The null lens and inspection microscope provided independent confirmation. Analysis of WFPC-2 images obtained during environmental testing in April-May 1993 showed that the Stimulus focus is within less than 0.1 mm of the average focus that had been independently established for the four channels of the flight instrument. The tests are discussed in detail elsewhere[8].

6. ACKNOWLEDGMENTS

We are grateful to numerous colleagues for their help in this work. We thank especially D. Ebbets, W. Conner, R. Debusk, E. Fuller, and D. Moody for technical assistance and V. Farmer for critical review of the reduction procedures. The Hartmann camera employed was designed by R. Chave, who served as Cognizant Engineer for the WFPC-2 Stimulus. The CCD system was provided by J. Trauger, Principal investigator for WFPC-2. The work described in this article was performed by the Jet Propulsion Laboratory, California Institute of Technology, under contract to the National Aeronautics and Space Administration.

7. REFERENCES

1. J. Hartmann, "Objektivuntersuchungen", Z *Instrumentenkd.* 24, 257, 1904; see also D. Malacara, A. Cornejo, and M. V. R. K. Murty, "Bibliography of various optical testing methods", ***Applied Optics*** **14,** 1065-1080, 1975.

2. A. H. Vaughan, N. A. Page, R. G. Chave, K. Almarzouk, and J. Rayces, "Optical design, fabrication, and alignment of a Hubble Space Telescope Simulator for Wide Field/Planetary Camera-II", paper 18, this conference. See also P. Davila, *et.al*, "Telescope simulators for Hubble: an overview of optical designs", ***Applied Optics*** 32, 1776, 1993.

3. J. R. Fienup, "Phase retrieval algorithms for a complicated optical system", *Applied Optics* ***32.1737,*** 1993.

4. The name "prescription retrieval" was proposed by Silas Brewer.

5. F. Roddier, "Variations on a Hartmann theme", *Optical Engineering* 29, 1239-1242, 1990,

6. M. Born and E. Wolf, "Principles of Optics", first edition, Permagon Press, p. ***374*** (footnote c), 1959.

7. C. J. Burrows, private communication, April, 1993

8. J. P. McGuire and R. J. Korechoff, "Optical alignment and ambient test of Wide Field/Planetary Camera-II", this conference.